

# Effect of Side Chain Length on Segregation of Squalane between Smectic Layers Formed by Rod-Like Polysilanes

Takuya Tanaka, Itsuki Kato and Kento Okoshi\*

Department of Applied Chemistry and Bioscience, Chitose Institute of Science and Technology, 758-65 Bibi, Chitose, Hokkaido 066-8655, Japan

**Abstract:** The segregation of spherical molecules (squalane) between the smectic layers of rod-like polymers (polysilanes) with narrow molecular weight distributions were investigated by synchrotron radiation small-angle X-ray scattering (SR-SAXS), atomic force microscopy (AFM) observations, and molecular dynamics simulations to elucidate the effect of the polymer side chain length on the segregation. It has been theoretically predicted that the smectic phase of the rod-like particles will be stabilized by inserting the spherical particles into the interstitial region between the smectic layers when the diameter of the spherical particles is smaller than that of the rod-like particles whose length is sufficiently long. We found that the segregation of squalane was unaffected by the molecular weight ( $M_w$ ) of the polysilane in the range of 9,200–44,100 g/mol, and the diameter of the polysilane showed the optimal size of 5.64 nm for the segregation of squalane whose diameter is 6.57 nm although the origin of these inconsistencies between theory and experiment is currently not clear.

**Keywords:** Helical polymer, liquid crystal, smectic phase, depletion effect, rod and sphere.

## 1. INTRODUCTION

The theoretical studies of liquid crystal (LC) formation have been extensively performed both by numerical calculations and computer simulations to elucidate the mechanism of the LC phase transitions. Some attempts have successfully reproduced the most commonly observed LC transition sequence of the nematic—smectic—columnar phases in the rod-like particles with a monodispersed length [1,2]. These theoretical predictions are in good agreement with the thermotropic LC phase behaviors of rigid-rod helical polysilanes with narrow molecular weight distributions [3,4], which are the only available systematic experimental studies for the LC phase behavior of hard-rod particle systems. This line of theoretical work developed into a wide variety of shapes of the rigid body, that is, spherical, disc-shaped [5], ellipsoidal [6], biaxial particles [7], and their mixtures, showing the possibility of discovering inconceivably unique LC structures. A typical example is the binary mixture of rod-like and spherical particles, showing the segregation of spherical particles between the smectic layers of the rod-like particles to expand the layer spacing and stabilize the smectic phase whereas the segregation competes with the bulk demixing [8,9]. Although various other inter-particle interactions are occurring among the particles, this theoretical prediction has been reproduced in some experimental binary systems, e.g., crystal nanorods and

nanospheres [10], gold nanorods and nanospheres [11], silica rods and spheres [12], and rod-like viruses and polystyrene latex or polyethylene oxide particles [13,14] when the diameters of the spheres are comparable or smaller than the diameter of the rods. On the other hand, the two components have been demixed from each other in some experimental binary systems [15,16] when the diameters of the spheres are sufficiently larger than the diameter of the rods. These results indicate that the relative size of the components plays a crucial role in the segregation, however, the sizes of the components in these systems could not be precisely controlled because they are produced by crystal growth or naturally produced in a virally infected *Escherichia coli* host, so that the systematic verification of the prediction by experiment has never been performed.

We recently reported the predicted segregation of squalane, a spherical branched alkane, between the smectic layers of a rigid-rod like helical polysilane with a narrow molecular weight distribution [17]. Polysilane is totally apolar and fully synthetic with a high degree of freedom for molecular design, which makes it possible to prepare a systematic series of ideal molecules for the experimental verification of theoretical predictions. Therefore, this system could expand the toolbox for the unexplored experiments because there still remain many unverified theoretical predictions.

In this study, we synthesized a series of rigid-rod like helical polysilanes with the different alkyl side chain carbon numbers of 6, 8, 10, and 12, designated as P6MS (poly[*n*-hexyl-(*S*)-2-methylbutylsilane]), P8MS

\*Address correspondence to this author at the Chitose Institute of Science and Technology, 758-65 Bibi, Chitose, Hokkaido 066-8655, Japan; Tel: +81-123-27-6084; Fax: +81-123-6084; E-mail: k-okoshi@photon.chitose.ac.jp

(poly[*n*-octyl-(*S*)-2-methylbutylsilane]), P10MS (poly[*n*-decyl-(*S*)-2-methylbutylsilane]), and P12MS (poly[*n*-dodecyl-(*S*)-2-methylbutylsilane]), respectively, to be added with squalane for the structural analyses of binary mixtures as illustrated in Figure 1. This allows us to confirm how the relative size of the components influence their assembly in the mixture, by comparing the actual size of each component estimated by molecular dynamic simulations.

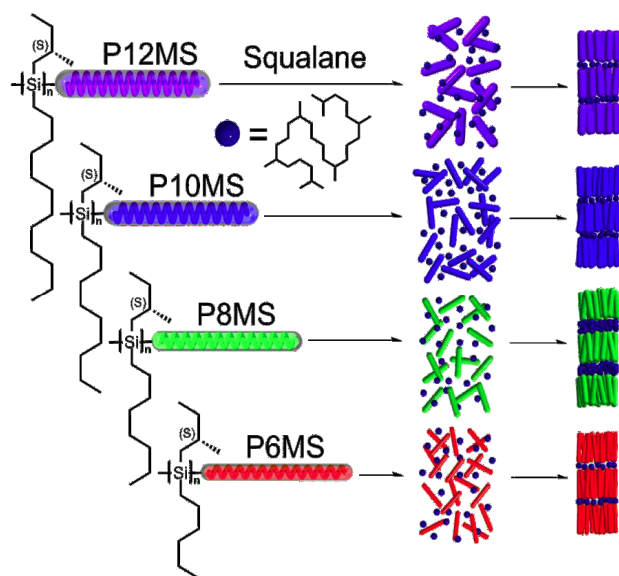


**Figure 1:** Schematic illustration of size effect on segregation of spherical molecules between smectic layers of rod-like polymers.

## 2. MATERIALS AND METHODS

The P<sub>n</sub>MSs were synthesized and fractionated by a fractional precipitation method to obtain samples with narrow molecular weight distributions according to the published method [18]. Squalane was obtained from Tokyo Chemical Industry Co., Ltd., and used without further purification. The molecular weights and molecular weight distributions of the P<sub>n</sub>MSs were determined by size exclusion chromatography (SEC) using a Lab solution GPC system (Shimadzu, Kyoto, Japan) equipped with two GPC K-805L columns (Showa Denko, Tokyo, Japan) with calibration by polystyrene standards (Showa Denko). Chloroform was used as the eluent at 40°C at the flow rate of 1 mL/min. The binary mixtures of P<sub>n</sub>MS and squalane were prepared by solution mixing in chloroform with the designated mixing ratios (weight of squalane / weight of binary mixture) followed by gradual evaporation of the solvent. High-resolution X-ray diffraction experiments for the P<sub>n</sub>MS/squalane mixtures were performed at the BL40B2of SPring-8 (Hyogo, Japan) with the approval

of the Japan Synchrotron Radiation Research Institute (JASRI) (Proposal No. 2015A1560 and 2015B1233) using a synchrotron radiation X-ray beam at a wavelength of 1.50 Å (8.00 keV) for the small-angle X-ray scattering (SAXS) and 1.00 Å (12.4 keV) for the wide-angle X-ray diffraction (WAXD) studies. The diffraction datasets were collected by a R-Axis VII imaging plate (Rigaku, Tokyo, Japan) with a camera length of 4000 mm and a 1-min X-ray exposure for the small-angle, and with a camera length of 500 mm and a 10-sec X-ray exposure for the wide-angle X-ray studies. High-resolution X-ray diffraction experiments for the molecular weight dependence of the P8MS/squalane mixtures were performed at the BL6A of the Photon Factory (Tsukuba, Japan) with the approval of the Photon Factory Program Advisory Committee (No. 2015G564) using a synchrotron radiation X-ray beam of 1.50 Å wavelength. The diffraction datasets were collected by a PILATUS3 1M (Dectris, Daettwil, Switzerland) with a camera length of 2500 mm and a 2-min X-ray exposure. AFM observations were carried out using a JSPM-5200 (JEOL, Ltd., Tokyo, Japan) in the AC-AFM mode at room temperature under ambient conditions. The samples for the AFM observations were prepared by spin-coating the chloroform solutions of the binary mixtures (2 mg/mL) on a glass substrate followed by exposure to chloroform vapor for 12 h. Molecular dynamics (MD) simulations were performed using SCIGRESS V2.7 (Fujitsu, Ltd., Tokyo, Japan) software with a LJDreiding force field. The helical main-chain structures of P<sub>n</sub>MS were assumed to be a 7-residue per 3 turn (7/3) helical conformation with the unit height of 0.198 nm for P6MS, 0.196 nm for P8MS, 0.194 nm for P10MS, and 0.196 nm for P12MS based on the WAXD studies. The series of polymer structures which satisfy the X-ray results were constructed with the bond angles (Si-Si-Si), bond lengths (Si-Si), and dihedral angles (Si-Si-Si-Si) calculated by Miyazawa's equation [19] employing the unit turn ( $2\pi \cdot 3/7$ ) and the unit heights, and evaluated the single point energies after geometry optimizations by molecular mechanics (MM) calculations with the MM3 force field with the backbone structures held fixed, so that the structure with the lowest total energy among these structures could be adopted as the initial structure for the MD simulations. The MD simulations were carried out in the NVT ensemble for 10 ps with a time step of 0.1 fs at 298 K with the initial structures of the P<sub>n</sub>MS 21mers with the main chain structure held fixed, employing the periodic boundary condition using the random cell of SCIGRESS with the density of 0.01 g/cm<sup>3</sup>. The MD

simulation of squalane was carried out in the same manner.

### 3. RESULTS AND DISCUSSION

The small- and wide-angle X-ray diffraction profiles of the binary mixtures of P8MS and squalane with various mixing ratios are shown in Figure 2. The smectic layer reflections in the small-angle region (Figure 2A) shifted to the small-angle direction whose spacing increased by 48.8% as the mixing ratio from 0 to 0.5 increased while the reflections in wide-angle region, which are attributed to a lateral packing of the polymer chain with the orthorhombic two-dimensional lattice of  $a = 1.57$  nm and  $b = 2.37$  nm as indexed in Figure 2B, remained in the almost same position whose unit cell area increased by only 1.02%. These clearly indicated that the selective segregation of the squalane between the smectic layers of P8MS took place without penetrating between the P8MS chains within the smectic layers although the wide-angle reflections gradually appeared upon the addition of squalane due to the structural relaxation of the

polymers within a smectic layer, which was just the same as those we had previously reported for P10MS [17]. It was also found that these behaviors were relatively unaffected by the molecular weight of P8MS (Figure 2C) in the range of 9,200–44,100 g/mol, whereas it has been theoretically predicted that the longer the length of the rods, the more the addition of spheres stabilized the smectic phase by layering them between the smectic layers to expand their layer spacings [9].

In Figure 3, the distribution ratio of squalane between and within the smectic layers in the binary mixtures with P6MS, P8MS, P10MS, and P12MS are shown, which were calculated by the following formulas for the distribution ratio of squalane between layers ( $R_{between}$ ):

$$R_{between} = (1 - r) \times \frac{\rho_{squalane}}{\rho_{PnMS}} \times \frac{L_r - L_0}{L_0} \times \frac{S_r}{S_0}$$

and for the distribution ratio of squalane within layers ( $R_{within}$ ):

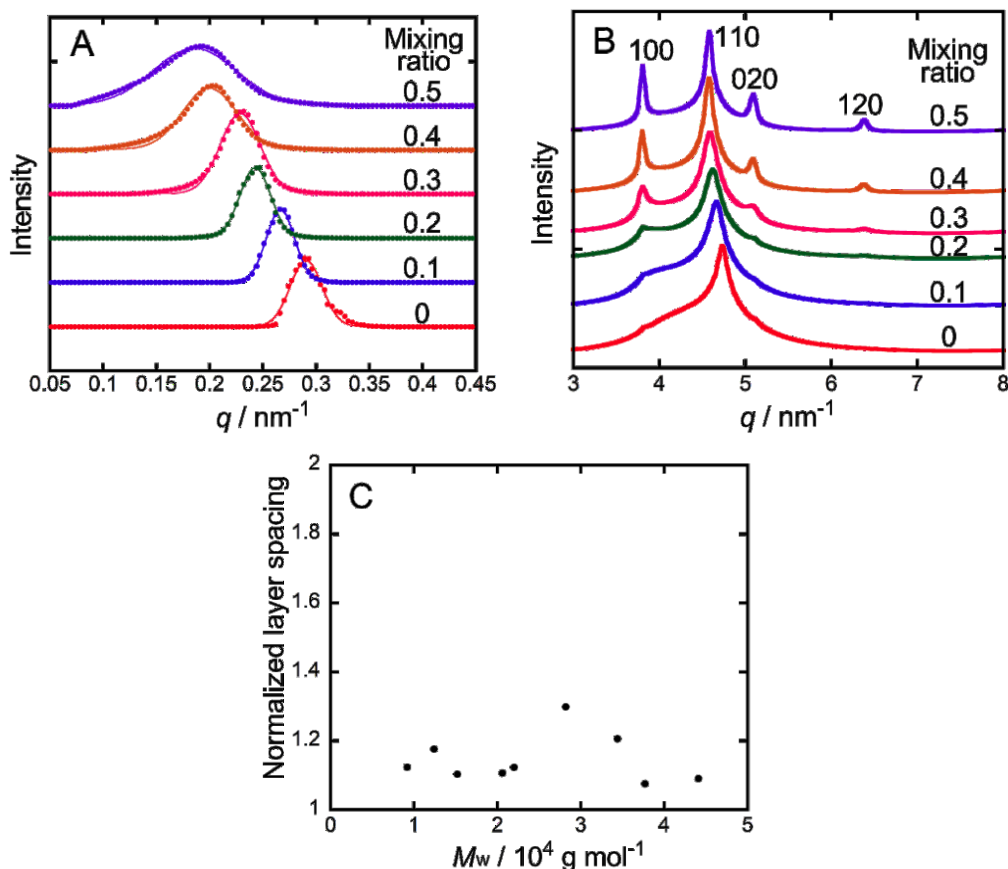


**Figure 2:** (A) Small- and (B) Wide-angle X-ray diffraction profiles of the mixtures of P8MS ( $M_w = 2.18 \times 10^4$ ,  $M_w/M_n = 1.16$ ) and squalane with various mixing ratios (weight of squalane / weight of binary mixture). The diffraction peaks are indexed on the basis of an orthorhombic two-dimensional lattice. (C) Molecular weight ( $M_w$ ) dependence of normalized layer spacing (layers spacing of binary mixture / layer spacing of polysilane) of binary mixtures of squalane and P8MS with the mixing ratio of 0.2.

$$R_{within} = (1-r) \times \frac{\rho_{squalane}}{\rho_{PnMS}} \times \frac{S_r - S_0}{S_0}$$

where  $r$  is the mixing ratio of squalane,  $\rho_{squalane}$  is the literature value of the squalane density, 0.808 g/cm<sup>3</sup>;  $\rho_{PnMS}$  is the density (g/cm<sup>3</sup>) of PnMS, 0.887 g/cm<sup>3</sup> for P6MS, 0.889 g/cm<sup>3</sup> for P8MS, 0.871 g/cm<sup>3</sup> for P10MS, and 0.879 g/cm<sup>3</sup> for P12MS, which were evaluated by the sink-float method;  $L_r$  is the smectic layer spacing (Å) of the PnMS/squalane mixture;  $L_0$  is the smectic layer spacing (Å) of PnMS;  $S_r$  is the orthorhombic unit cell area (Å<sup>2</sup>) of the PnMS/squalane mixture; and  $S_0$  is the orthorhombic unit cell area (Å<sup>2</sup>) of PnMS.

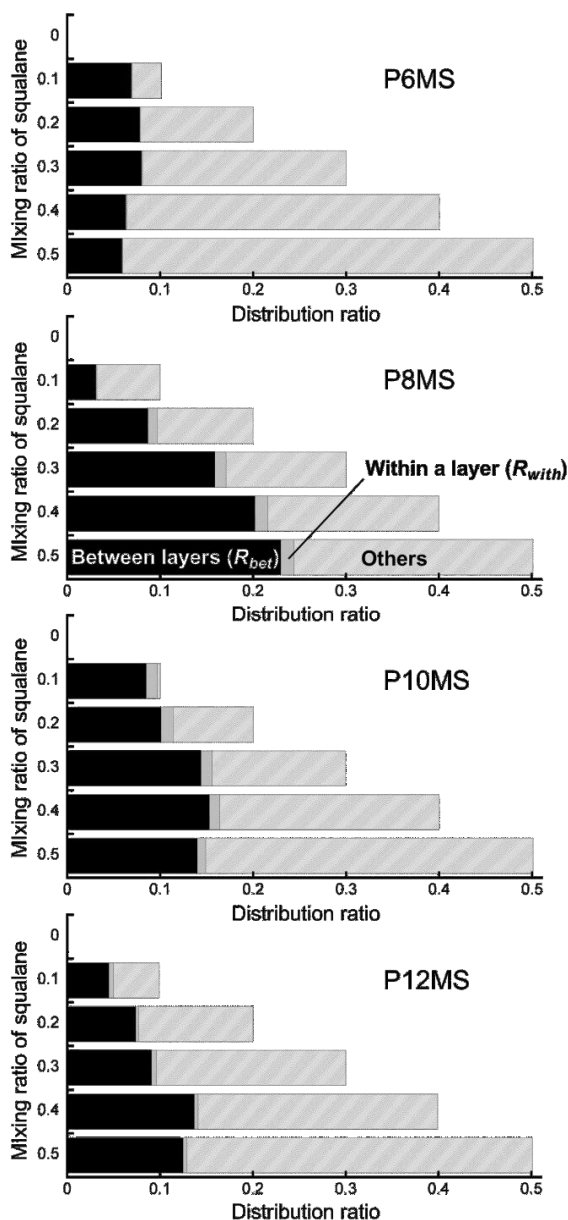


**Figure 3:** Distribution ratios of the squalane between and within the smectic layers in the mixtures with P6MS, P8MS, P10MS, and P12MS.

The squalane was more or less selectively segregated between the smectic layers without penetrating into the smectic layers even in the binary mixtures with P6MS and P12MS, while the rest of the squalane was considered to be forced out of the liquid crystal domain and absorbed in the domain boundary because no sign of microscopic phase separation was found by polarized optical microscopic observations. Upon increasing the mixing ratio, the amount of the squalane segregated between the smectic layers reached a plateau at around the mixing ratio of 0.3 or 0.4 for the binary mixtures with P6MS, P10MS, and P12MS; however, it monotonously increased in the binary mixture with P8MS in which nearly half of the squalane was segregated between the smectic layers. This might be due to the enthalpic attraction force between the polymers with longer or shorter sidechains because the amount of squalane that penetrated within a smectic layer is significantly low in P6MS and P12MS.

This segregation behavior was further investigated by AFM observations by which the smectic layer structure and its order can be clearly elucidated. Figure 4 shows the AFM images and corresponding 2-dimensional Fourier transform of the binary mixtures of P8MS and squalane spin-cast on the glass substrates with the various mixing ratios. Clear banding patterns, which are attributed to the smectic layers, can be observed. The distance between the banding was monotonically expanded with the increasing mixing ratio, as has been previously observed in the binary mixture with P10MS; however, it was non-uniformly broadened at the mixing ratio of 0.4, which is consistent with the broadening of the corresponding smectic layer reflection in Figure 2A. The banding distance was partially widened more than 5 times thicker than its pristine P8MS, which is fully consistent with the theoretical prediction that the periodicity of the smectic phase increases to the maximum limit of the bulk demixing as the volume fraction of the spheres increases [9].

Due to the fact that this broadening of the smectic layer spacing is significant, especially in P8MS, while less prominent in the rest of the polysilanes, one can predict that there is an optimal relative size for the rod-like and spherical molecules, which might play a crucial role in the structural formation and segregation.

In light of these experimental results, we evaluated the size of these components of the mixtures based on the molecular dynamics simulations. After the

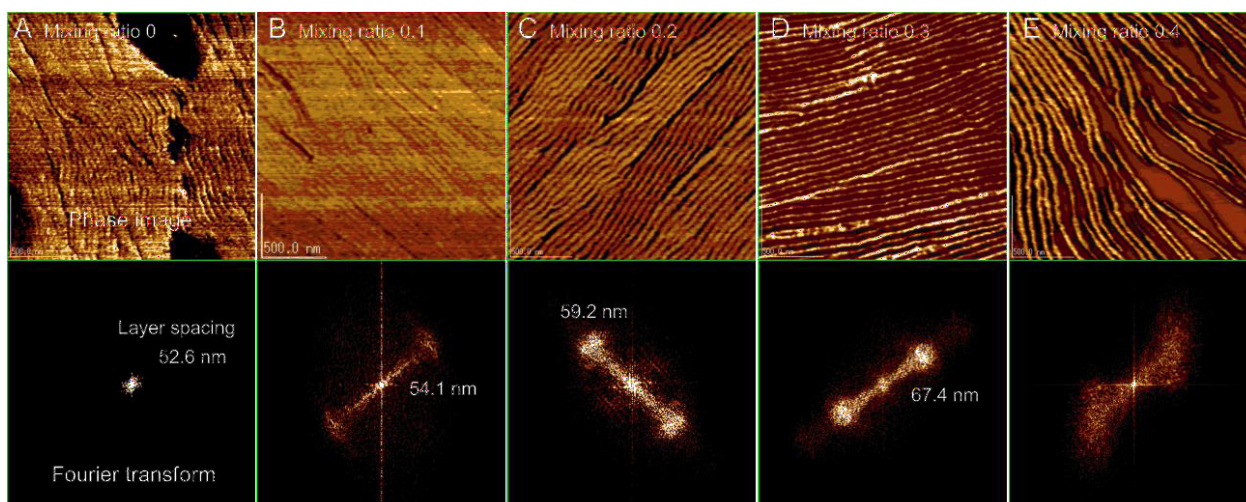


**Figure 4:** AFM images and corresponding Fourier transforms observed on the film of binary mixtures of P8MS ( $M_w = 1.33 \times 10^5$ ,  $M_w/M_n = 1.55$ ) and squalane at the mixing ratios (squalane/mixture) of (A) 0, (B) 0.1, (C) 0.2, (D) 0.3, and (E) 0.4 spin-coated on the glass substrates. Scale =  $2 \times 2 \mu\text{m}$ .

simulations were performed in the manner described in the experimental section, the central 7mers of the calculated PnMS 21mers were extracted every 0.1 ps in the last 3 ps where they are in equilibrium to avoid any influence from the end groups. The radius of gyration of PnMS around the main chain axis and that of squalane were then calculated by the following formulas for PnMS with the main chain aligned in the direction of the z-axis:

$$\langle S^2 \rangle = \frac{\sum_i m_i (x_i^2 + y_i^2)}{\sum_i m_i}$$

and for squalane:

$$\langle S^2 \rangle = \frac{\sum_i m_i (x_i^2 + y_i^2 + z_i^2)}{\sum_i m_i}$$

The equilibrium structures and estimated radius of gyrations of PnMSs and squalane are shown in Figure 5. The radius of gyrations of squalane was between those of P8MS and P10MS, rather close to P10MS, although the accuracy of the estimation could be questioned because the mean radius of gyration of these components in the solid state should be smaller than those in a vacuum. It should be necessary to expand the variety of the side chain lengths for more detailed analyses, however, the variation in the alkyl sidechain is technically limited. The PnMSs lose their main chain rigidity and never formed a liquid crystal phase with the alkyl sidechain length of less than 4, while the alkyl sidechain crystallizes when its length is greater than 15. Therefore, it might be preferable to employ a series of spherical molecules with different radii of gyration other than squalane to cover the wide

variety of relative sizes, because squalane is naturally sourced and has almost no room for molecular design.

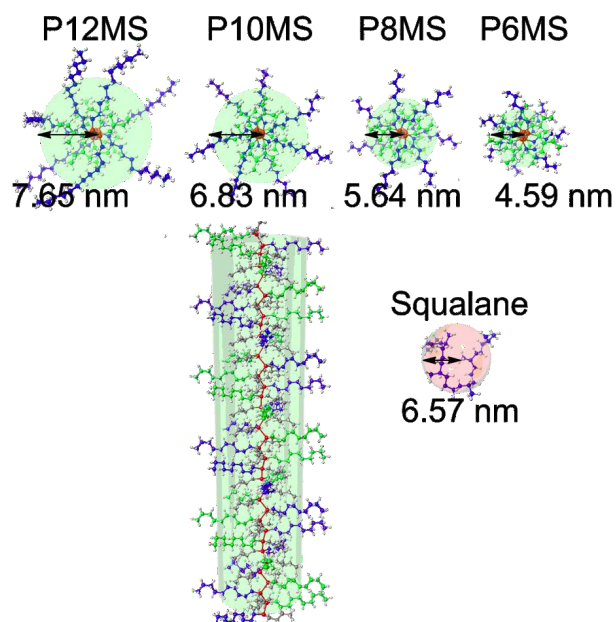


**Figure 5:** Equilibrium structures and calculated mean radius of gyration of PnMSs and squalane.

#### 4. CONCLUSION

We performed the structural analyses of the binary mixtures of rod-like polymers (PnMSs) and a spherical molecule (squalane) and found that the predicted insertion of spheres between the smectic layers of the rods was significantly influenced by the relative size of the components which showed an optimal size; the insertion of the spheres is limited if the diameter of the squalane is larger/smaller than the optimal size. These results are not consistent with the theoretical results

which predicted that the decrease in the sphere size stabilizes the smectic layered structure [9]. Even though the origin of this inconsistency is not clear, it might be suggested that the increase or decrease in the sidechain length of the polysilane increases the attraction force between the polymers in terms of the enthalpic effects, which should be inconsistent with the predicted entropic segregation in the athermal systems.

We have also shown that the segregation of the spherical molecule between the smectic layers of the rod-like polymers exhibited a line pattern when cast on the substrate with a variable width and gap regulated by the molecular weight of the polymer and the mixing ratio of the spherical molecule. This indicated the possibility of using this structure as a template for metal-patterning as has been considered to be manufactured with the lamella structure of a block copolymer. Considering the fact that the polysilane can be highly aligned on the rubbed polyimide alignment layer [20], this can be used as an anisotropically conductive film or polarizers, and the studies along these lines are in progress.

## ACKNOWLEDGEMENTS

This study was supported by JSPS KAKENHI Grant Number JP16K04867, JP17K06033, and the Nanotechnology Platform Program (Synthesis of Molecules and Materials) of the Ministry of Education, Culture, Sports, Science and Technology (MEXT), Japan.

## REFERENCES

- [1] Stroobant A, Lekerkerker HNW, Frenkel D. Evidence for Smectic Order in a Fluid of Hard Parallel Spherocylinders. *Phys Rev Lett* 1986; 57: 1452-1455. <https://doi.org/10.1103/PhysRevLett.57.1452>
- [2] Stroobant A, Lekerkerker HNW, Frenkel D. Evidence for one-, two-, and three-dimensional order in a system of hard parallel spherocylinders. *Phys Rev A* 1987; 36: 2929-2945. <https://doi.org/10.1103/PhysRevA.36.2929>
- [3] Okoshi K, Kamee H, Suzaki G, Tokita M, Fujiki M, Watanabe J. Well-Defined Phase Sequence Including Cholesteric, Smectic A, and Columnar Phases Observed in a Thermotropic LC System of Simple Rigid-Rod Helical Polysilane. *Macromolecules* 2002; 35: 4556-4559. <https://doi.org/10.1021/ma012056z>
- [4] Okoshi K, Saxena A, Naito M, Suzaki G, Tokita M, Watanabe J, Fujiki M. First observation of a smectic A-cholesteric phase transition in a thermotropic liquid crystal consisting of a rigid-rod helical polysilane. *Liq Cryst* 2004; 31: 279-283. <https://doi.org/10.1080/02678290410001648598>
- [5] Veerman JAC, Frenkel D. Phase behavior of disklike hard-core mesogens. *Phys Rev A* 1992; 45: 5632-5648. <https://doi.org/10.1103/PhysRevA.45.5632>
- [6] Frenkel D, Moulder BM, McTague JP. Phase Diagram of a System of Hard Ellipsoids. *Phys Rev Lett* 1984; 52: 287-290. <https://doi.org/10.1103/PhysRevLett.52.287>
- [7] Michael PA. Computer simulation of a biaxial liquid crystal. *Liq Cryst* 1990; 8: 499-511. <https://doi.org/10.1080/02678299008047365>
- [8] Koda T, Numajiri M, Ikeda S. Smectic-A Phase of a Bidisperse System of Parallel Hard Rods and Hard Spheres. *J Phys Soc Jpn* 1996; 65: 3551-3556. <http://journals.jps.jp/doi/10.1143/JPSJ.65.3551>
- [9] Dogic Z, Frenkel D, Fraden S. Enhanced stability of layered phases in parallel hard spherocylinders due to addition of hard spheres. *Phys Rev E* 2000; 62: 3925-3933. <https://doi.org/10.1103/PhysRevE.62.3925>
- [10] Ye X, Millan JA, Engel M, Chen J, Diroll BT, Glotzer SC, Murray CB. Shape Alloys of Nanorods and Nanospheres from Self-Assembly. *Nano Lett* 2013; 13: 4980-4988. <https://doi.org/10.1021/nl403149u>
- [11] Ahmad I, Zandvliet HJW, Kooij ES. Shape-Induced Separation of Nanospheres and Aligned Nanorods. *Langmuir* 2014; 30: 7953-7961. <https://doi.org/10.1021/la500980j>
- [12] Bakker HE, Dussi S, Droste BL, Besseling TH, Kennedy CL, Wiegant EI, Liu B, Imhof A, Dijkstra M, van Blaaderen A. Phase diagram of binary colloidal rod-sphere mixtures from a 3D real-space analysis of sedimentation-diffusion equilibria. *Soft Matter* 2016; 12: 9238-9245. <https://doi.org/10.1039/C6SM02162J>
- [13] Adams M, Fraden S. Phase Behavior of Mixtures of Rods (Tobacco Mosaic Virus) and Spheres (Polyethylene Oxide, Bovine Serum Albumin). *Biophys J* 1998; 74: 669-677. [https://doi.org/10.1016/S0006-3495\(98\)77826-9](https://doi.org/10.1016/S0006-3495(98)77826-9)
- [14] Adams M, Dogic Z, Keller SL, Fraden S. Entropically driven microphase transitions in mixtures of colloidal rods and spheres. *Nature* 1998; 393: 349-352. <https://doi.org/10.1038/30700>
- [15] Koenderink GH, Vliegthart GA, Kluijtmans SGJM, van Blaaderen A, Philipse AP, Lekkerkerker HNW. Depletion-Induced Crystallization in Colloidal Rod-Sphere Mixtures. *Langmuir* 1999; 15: 4693-4696. <https://doi.org/10.1021/la990038t>
- [16] Yasarawan N, van Duijneveldt JS. Arrested phase separation of colloidal rod-sphere mixtures. *Soft Matter* 2010; 6: 353-362. <https://doi.org/10.1039/B915886C>
- [17] Tanaka T, Kato I, Okoshi K. Nano-Segregation of Squalane between Smectic Layers of Rigid-Rod Polysilane. *e-J Sur Sci Nanotech* 2015; 13: 121-124. <https://doi.org/10.1380/ejssnt.2015.121>
- [18] Fujiki M. A Correlation between Global Conformation of Polysilane and UV Absorption Characteristics. *J Am Chem Soc* 1996; 118: 7424-7425. <https://doi.org/10.1021/ja953835w>
- [19] Miyazawa T. Molecular vibrations and structure of high polymers. II. Helical parameters of infinite polymer chains as functions of bond lengths, bond angles, and internal rotation angles. *J Polym Sci* 1961; 55: 215-231. <https://doi.org/10.1002/pol.1961.1205516121>
- [20] Okoshi K, Fujiki M, Watanabe J. Asymmetrically Tilted Alignment of Rigid-Rod Helical Polysilanes on a Rubbed Polyimide Surface. *Langmuir* 2012; 28: 4811-4814. <https://doi.org/10.1021/la204789g>